Technical Report Documentation Page

1. Report No. FHWA/TX-7-2957-1	2. Government Accession No.	3. Recipient's Catalog No.
4. Title and Subtitle IMPROVING THE ACOUSTICAL PERFORMANCE OF POROUS ASPHALT PAVEMENTS		5. Report Date September 1999
7. Author(s) Jeffrey DeMoss, B. J. Landsberger, and Michael T. McNerney		6. Performing Organization Code 8. Performing Organization Report No. 2957-1
9. Performing Organization Name and Address Center for Transportation Research The University of Texas at Austin 3208 Red River, Suite 200 Austin, TX 78705-2650		10. Work Unit No. (TRAIS) 11. Contract or Grant No. Research Study 7-2957
12. Sponsoring Agency Name and Address Texas Department of Transportation Research and Technology Transfer Section/Construction Division P.O. Box 5080 Austin, TX 78763-5080		13. Type of Report and Period Covered Research Report (9/98–8/99) 14. Sponsoring Agency Code

15. Supplementary Notes
Project conducted in cooperation with the Texas Department of Transportation.

16. Abstract

Selection of pavement for noise reduction considerations is becoming a major concern for those involved in highway construction within densely populated areas. However, the pavements available are designed for durability and safety reasons and not for their acoustic characteristics. The purpose of this study is to develop a pavement design criterion for improved acoustical performance. Existing porous media theory can be used to predict the absorption characteristics of asphalt pavements. Experiments and theoretical analysis were performed on test pavement samples to determine the acoustical characteristics of different pavement mixes where aggregate size, pavement layer thickness, percent of air voids, mix of aggregates and amount of screenings were varied. Tests were conducted on both single and multiple-layer pavement laboratory samples. Good agreement was found between the predicted and measured values of absorption. It is shown that by varying the thickness of the pavement layers the peak value of absorption can be matched to achieve maximum noise reduction at the frequencies where traffic noise is most prominent.

17. Key Words Acoustical absorption, porous asphalt, noise reduction	18. Distribution Statement No restrictions. This document is available to the public through the National Technical Information Service, Springfield, Virginia 22161.

19. Security Classif. (of report) Unclassified	20. Security Classif. (of this page) Unclassified	21. No. of pages 54	22. Price

Form DOT F 1700.7 (8-72) Reproduction of completed page authorized

IMPROVING THE ACOUSTICAL PERFORMANCE OF POROUS ASPHALT PAVEMENTS

by

Jeffrey DeMoss, B.J. Landsberger, and Michael T. McNerney

Research Report Number 2957-1

Research Project 7-2957

Project Title: Use of Pavement Surfaces to Attenuate Traffic Noise

Conducted for the

TEXAS DEPARTMENT OF TRANSPORTATION

by the

CENTER FOR TRANSPORTATION RESEARCH

Bureau of Engineering Research

THE UNIVERSITY OF TEXAS AT AUSTIN

September 1999

DISCLAIMERS

The contents of this report reflect the views of the authors, who are responsible for the facts and the accuracy of the data presented herein. The contents do not necessarily reflect the official views or policies of the Texas Department of Transportation. This report does not constitute a standard, specification, or regulation.

There was no invention or discovery conceived or first actually reduced to practice in the course of or under this contract, including any art, method, process, machine, manufacture, design or composition of matter, or any new and useful improvement thereof, or any variety of plant, which is or may be patentable under the patent laws of the United States of America or any foreign country.

NOT INTENDED FOR CONSTRUCTION,
BIDDING, OR PERMIT PURPOSES

Dr. Michael T. McNerney, P.E. (Texas No. 70176)
Research Supervisor

ACKNOWLEDGMENTS

The researchers thank TxDOT Project Director Gary Graham (DES) for his direction and facilitation of the research. The assistance of the other members of the project monitoring committee, which included C. Herrera (CST), M. Shearer (ENV), and P. Henry (HOU) is also appreciated. Special thanks are also extended to Gulanini Kanthasamy and to the support crew at TxDOT Superpave Laboratory for assistance in the test sample preparation. Finally, the researchers express appreciation to Dr. Mark Hamilton, Dr. Elmer Hixson, and Dr. Elmira Popova at The Univeristy of Texas at Austin for their academic expertise and for their contribution to the testing and analysis portion of the research.

Research performed in cooperation with the Texas Department of Transportation

TABLE OF CONTENTS

CHAPTER 1 . INTRODUCTION

1.1 PROJECT OBJECTIVE

As urban areas become more densely populated, communities will continue to seek cost-effective ways to reduce noise pollution. Recent data relating pavement type and road noise suggest that certain pavement designs are responsible for reducing measured noise levels.[1] These pavements tend to be constructed with a more porous aggregate mixture than that used in traditional pavements. Previous work has shown that the asphalt structure can be modeled acoustically using established acoustical theory for porous media.[2] This theory can be used to predict a noise absorption coefficient that can be measured experimentally using standard laboratory techniques. The purpose of this study is to develop a method for pavement design that uses noise absorption performance as the primary design criterion.

1.2 PREVIOUS WORK

There have been several articles published during the last decade covering noise measurements of different pavement surfaces.[1,3,4] Generally they have found that porous asphalt pavements have lower noise levels compared to other surfaces under similar traffic conditions. Experiments by Iwai et al.[5] indicated that for porous asphalt pavements less noise is radiated at the tire road contact area and that less noise is transmitted along the road surface. The Center for Transportation Research conducted roadside and tire noise measurements along fifteen different pavement surfaces in Texas.[3] The data were collected from two microphones that recorded the drive-by noise produced by a test vehicle. The results from this survey are presented in Table 1.1. A notable result was the performance of the aged Novachip. This is a commercial pavement surface overlay with a relatively porous structure. Other data taken in South Africa using a similar roadside test show a significant reduction in noise using another porous pavement design commercially known as "Whisper Course".[4] These results are shown in Table 1.2.

TABLE 1.1. *Recorded noise levels with Texas pavements.*

Pavement	Roadside SPL (dBA)		
	Average	Left Channel	Right Channel
Nova Chip (Aged)	80.4	80.2	80.7
Microsurfacing (N. Mopac)	80.5	79.9	81.2
CMHB	81.4	81.1	81.6

Asphalt (New)	81.8	82.2	81.5
Nova Chip (New)	82.5	83.0	82.0
JRCP (Ungrooved)	83.1	82.9	83.4
Microsurfacing (Corpus)	83.4	83.5	83.2
CRCP (Untined)	83.5	84.0	82.9
Asphalt (Aged)	83.6	83.7	83.4
Chip Seal (Grade 4)	84.9	84.8	85.1
CRCP (Aged)	85.1	85.6	84.6
CRCP(New)	85.1	85.1	85.0
Aged Asphalt (Control)	85.5	84.7	86.3
JRCP (Grooved)	86.3	86.8	85.8
Asphalt (Grooved)	87.2	87.7	86.8

TABLE 1.2*. Recorded noise levels of South African pavements.*

Pavement	Roadside SPL dBA
Seal Coat (13 mm (0.05 in.))	89.4
Jointed Concrete	89.0
Seal Coat (19 mm (0.075 in.))	84.5
Dense Graded Asphalt	79.8
Open Graded Asphalt	79.7
Whisper Course	77.2

Although the noise reduction measured in tire noise tests[3] is significant for porous asphalt, the physics responsible for the decrease in the measured SPL are not fully understood. The data suggest that less noise is generated at the tire/pavement contact area of more porous asphalt. This may be a result of noise being absorbed at the source due to the acoustical absorption properties of the pavement itself. Berengier et al.[2] showed successfully that the acoustical absorption properties of pavement could be modeled using standard porous media theory. Their findings offer some explanation for the improved acoustical performance of more porous asphalt over standard pavement designs.

1.3 SUMMARY

The body of this report begins with an overview of the theory used by Berengier et al.[2] to predict the acoustical absorption coefficient of porous asphalt. The current theory considers only a single layer of porous material. Since practical pavement designs often consist of multiple layers, the model was extended to include an additional layer of porous material.

Two standard techniques for measuring acoustical absorption are the impedance tube method and the reverberation room method. The impedance tube measures a noise absorption coefficient for waves at normal incidence that can be compared directly to the theoretical predictions. The reverberation room method measures absorption in a diffuse

field. A diffuse sound field more accurately represents noise-pavement interaction under real conditions. Since different values for the absorption coefficient are expected when comparing the two methods, both techniques were implemented. Although the purpose of this study is not to compare the two measurement techniques, some insight may be gained by examining differences between the two methods. Chapters 3 and 4 explain the experimental setup and results for each technique. Also included are details of the manufacturing of the asphalt samples used in the experiments.

Chapter 5 explains how the findings of the study may be applied to the design of porous asphalt. The report concludes with recommendations for future work.

CHAPTER 2 . APPLICATION OF POROUS MEDIA THEORY TO PAVEMENT

2.1 SINGLE-LAYER DERIVATION

Reviewed below is the derivation of the porous media theory used by Berengier et al.[2] as applied to porous asphalts. It is assumed that the pavement structure consists of two acoustical materials. The first is a solid structure made of the aggregate, screenings, and asphalt. The second assumption is that air exists in the voids of the sample. It is further assumed that sound waves arrive at normal incidence and are one-dimensional. The solid layer is assumed to have an acoustic impedance much higher than air, and therefore waves in the solid are ignored. All sound entering the sample is assumed to propagate only through the air voids in the sample. Any air voids that are isolated by the solid do not contribute to sound propagation. Thus only the communicating voids are considered when determining the porosity of a pavement sample. A further assumption is that the physical properties, including porosity, airflow resistivity, and shape factor are uniform through the thickness of the sample. The theory is limited to frequencies that have wavelengths that are large compared to the size of the voids and aggregate. For typical samples, the characteristic dimension of the voids and aggregate is on the order of 5 mm (0.02 in.), an equivalent wavelength for which corresponds to a frequency of 68 kHz. The theory is used here for frequencies far below that limit.

Beginning with the continuity and momentum equations defined by Attenborough,[6] one derives a wave equation by making a small signal assumption for the corresponding one-dimensional continuity and momentum equations:

$$\Omega \frac{\partial \rho}{\partial t} + \rho_0 \frac{\partial u}{\partial x} = 0 \qquad (2.1)$$

and

$$\rho_0 \frac{K}{\Omega} \frac{\partial u}{\partial t} + R_S u = -\frac{\partial p}{\partial x} \qquad (2.2)$$

where u is the average particle velocity, ρ is the instantaneous (total) density, and p is the sound pressure. Here ρ_0 and c_0 are the equilibrium density and the adiabatic velocity of sound in air, respectively. The wave equation for a perfectly rigid porous medium then takes the form of

$$\frac{\partial^2 p}{\partial x^2} - \frac{K}{c_0^2} \frac{\partial^2 p}{\partial t^2} - \frac{R_s \Omega}{\rho_0 c_0^2} \frac{\partial p}{\partial t} = 0 \ . \qquad (2.3)$$

The three constants porosity Ω, resistivity R_s, and shape factor K are parameters that define the physical properties of the medium. Porosity is the volume fraction of communicating pores, such that

$$\Omega = \frac{\text{volume of communicating voids}}{\text{total volume}} \ . \qquad (2.4)$$

Airflow resistance R_s is a DC flow resistivity constant that describes how easily air can pass through the sample. It is defined as

$$R_S = \frac{1}{u_\ell}\frac{\Delta P}{\ell}, \qquad (2.5)$$

where u_ℓ is the steady volume flow rate and ΔP is the pressure difference between the two faces of the porous layer of thickness ℓ. Air paths through the porous layer usually follow an indirect or tortuous route. The result is that the effective signal path through the sample medium is longer than the thickness of the porous layer. A shape factor K is introduced to account for the increase in propagation distance. Harmonic motion $e^{i\omega t}$ is assumed, such that a solution takes the form

$$p = Ae^{i(\omega t - k_s x)}. \qquad (2.6)$$

Substituting into Eq. (2.3) and solving for k_s yields

$$k_s = \frac{\omega}{c_0}\sqrt{K}\left(1 - i\frac{R_s\Omega}{\omega\rho_0 K}\right)^{1/2} \ . \qquad (2.7)$$

The characteristic impedance of the sample layer is found by using the relation for impedance of a progressive plane wave, $Z = p/u$. The momentum equation together with Eqs. (2.6) and (2.7) are used to obtain

$$Z_s = \rho_0 c_0 \frac{\sqrt{K}}{\Omega}\left(1 - i\frac{R_s\Omega}{\omega\rho_0 K}\right)^{1/2} \ . \qquad (2.8)$$

The acoustic absorption coefficient α is the ratio of the absorbed acoustic energy to the total energy impacting the surface. In terms of the pressure reflection coefficient *R*, it is defined by $\alpha = 1 - |R|^2$. The theory makes use of the solution of the pressure reflection coefficient for a three-media problem as shown in Figure 2.1.[7]

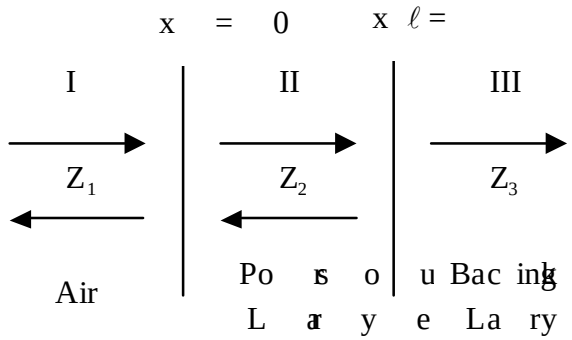

Figure 2.1. Incident, reflected and transmitted wave fields for a three-media problem.

The pressure fields in Figure 2.1 are described as follows:

$$\begin{aligned} &\text{I: } P_1 = A_1 e^{-jk_1 x} + B_1 e^{jk_1 x}\ , \\ &\text{II: } P_2 = A_2 e^{-jk_2 x} + B_2 e^{jk_2 x}\ , \\ &\text{III: } P_3 = A_3 e^{-jk_3 (x-\ell)}, \end{aligned} \tag{2.9}$$

where k_i is the wave number with the subscript corresponding to the layer and ℓ is the thickness of layer II.

The pressure reflection coefficient can be determined by using Eqs. (2.9) and matching the pressures and particle velocities at the two boundaries ($x = 0, \ell$):

$$R = \frac{\left(1 - \dfrac{Z_1}{Z_3}\right)\coth k_2\ell + \dfrac{Z_2}{Z_3} - \dfrac{Z_1}{Z_2}}{\left(1 + \dfrac{Z_1}{Z_3}\right)\coth k_2\ell + \dfrac{Z_2}{Z_3} + \dfrac{Z_1}{Z_2}}\ . \tag{2.10}$$

If layer I is air, $Z_1 = \rho_0 c_0$, Eq. (2.10) can be arranged in the form:

$$R = \frac{Z - \rho_0 c_0}{Z + \rho_0 c_0}, \tag{2.11}$$

where

$$Z = Z_s \frac{Z_T \coth ik_s\ell + Z_s}{Z_T + Z_s \coth ik_s\ell}\ . \tag{2.12}$$

Z_T is the impedance of the backing layer, and k_i and Z_s are the wave number and impedance of the sample, respectively. The equation for the absorption coefficient then becomes

$$\alpha = 1 - \frac{|Z - \rho_0 c_0|^2}{|Z + \rho_0 c_0|^2} \ . \qquad (2.13)$$

Under normal testing conditions, the backing layer is metal; therefore, Eq. (2.12) may be simplified by assuming $Z_T = \infty$. Thus, α is frequency dependent and determined by the four parameters: thickness ℓ, porosity Ω, airflow resistivity R_S, and shape factor K.

Figure 2.2 shows an example of the theoretical predictions of α for an absorptive pavement. The peaks observed in the graph are typical of all porous media, and they repeat periodically with increasing frequency as shown by the 2 in. sample in the graph. Berengier et al.[2] found that varying Ω changes the maximum value of α when plotted versus frequency. Increasing R_S tends to reduce the peaks and raise the minima of the absorption. K and ℓ determine the frequency at which the absorption peaks occur. Since the frequency for maximum absorption is dependent on the thickness, it is possible to design a pavement layer to achieve maximum absorption around a desired frequency. Ideally, this would be in the frequency range where traffic noise contains the most energy. The curves were generated using $\Omega = 0.254$, R_S=38000 N-s/m^4 and K=3.7.

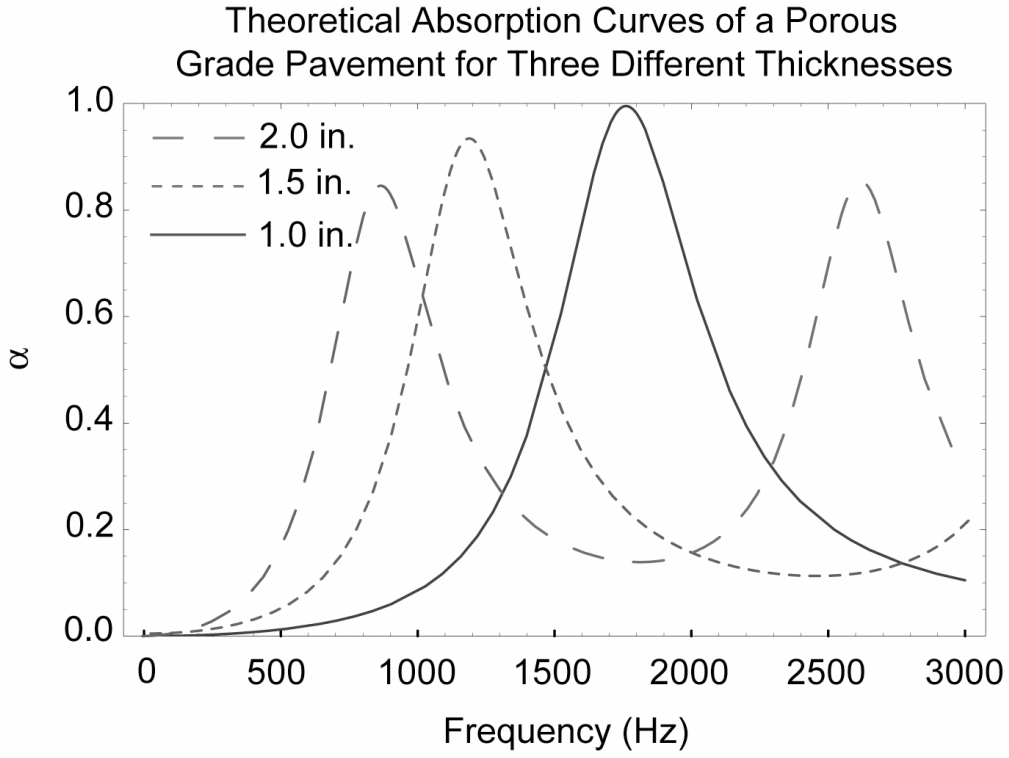

Figure 2.2. Graph showing theoretical prediction of the absorption curves of a typical porous grade pavement, for three different thicknesses.

2.2 DOUBLE-LAYER DERIVATION

In order to model multiple-layer pavement samples, the single-layer theory can be extended to include a second porous layer. More realistic pavements may be designed to have a porous overlay on top of a dense-grade existing pavement. A graphical depiction of the wave field for a double-layer sample is shown in Figure 2.3.

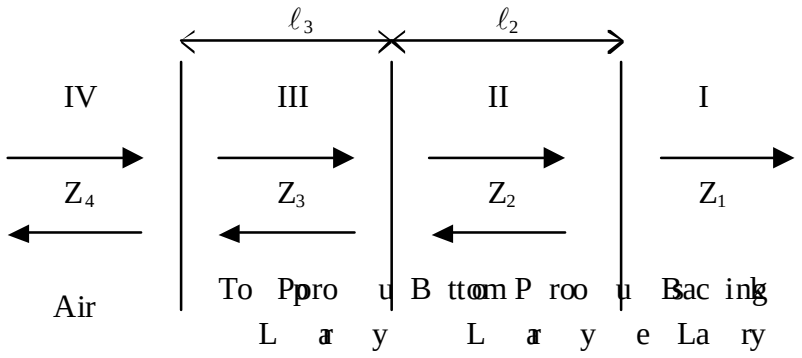

Figure 2.3. Incident, reflected and transmitted wave fields for a four-media problem.

The same wave equation used to derive the single-layer theory applies to derivation of the multiple-layer theory. The pressure reflection coefficient can be found by applying a theory of layered media such as the one found in the text by Brekhovskikh and Godin.[8] The solution is obtained by using the following equation recursively:

$$Z_{in}^{(n)} = Z_n \frac{Z_{in}^{(n-\ell)} - iZ_n \tan(k_n \ell_n)}{Z_n - iZ_{in}^{(n-\ell)} \tan(k_n \ell_n)}, \tag{2.14}$$

where $Z_{in}^{1} = Z_1$. The above equation for Z_{in}^{n}, where n –1 is the number of layers, is used to find the pressure reflection coefficient such that

$$R = \frac{Z_{in}^{(n)} - Z_{n+1}}{Z_{in}^{(n)} + Z_{n+1}} \ . \tag{2.15}$$

For $Z_4 = \rho_0 c_0$, and with a backing layer impedance of infinity ($Z_1 = \infty$), the absorption coefficient is found in terms of the physical parameters of both porous layers:

$$\alpha = 1 - \frac{|\, Z_{in}^{3} - \rho_0 c_0 \,|^2}{|\, Z_{in}^{3} + \rho_0 c_0 \,|^2}, \tag{2.16}$$

where

$$Z_{in}^3 = Z_3 \frac{Z_{in}^2 - iZ_3 \tan(k_3 \ell_3)}{Z_3 - iZ_{in}^2 \tan(k_3 \ell_3)}, \tag{2.17}$$

$$Z_{in}^2 = iZ_2 \frac{1}{\tan(k_2 \ell_2)}, \tag{2.18}$$

$$Z_3 = \frac{\rho_0 c_0}{\Omega_3} \sqrt{K_3} \left(1 - \frac{iR_3 \Omega_3}{\omega \rho_0 K_3} \right)^{1/2}, \tag{2.19}$$

$$Z_2 = \frac{\rho_0 c_0}{\Omega_2} \sqrt{K_2} \left(1 - \frac{iR_2 \Omega_2}{\omega \rho_0 K_2} \right)^{1/2}, \tag{2.20}$$

$$k_3 = \frac{\omega}{c_0} \sqrt{K_3} \left(1 - i \frac{R_3 \Omega_3}{\omega \rho_0 K_3} \right)^{1/2}, \tag{2.21}$$

and

$$k_2 = \frac{\omega}{c_0} \sqrt{K_2} \left(1 - i \frac{R_2 \Omega_2}{\omega \rho_0 K_2} \right)^{1/2}. \tag{2.22}$$

Note that Eqs. (2.14), (2.17), and (2.18) can be written in hyperbolic cotangent form to resemble Eq. (2.12) using the relation $\cot(x) = i \coth(ix)$.

CHAPTER 3 . IMPEDANCE TUBE TESTS AND RESULTS

This chapter begins with a description of the impedance tube and the test equipment used in the experiments. Also outlined below is the method for calculating the absorption coefficients from the measured data. Tests were done on a variety of different pavement samples to determine how changes in aggregate mixture and sample dimensions affect the measured absorption coefficient. A description of the construction of the test samples is also included. The test results are presented in two sections, one each for single-layer results and double-layer results.

3.1 TEST SETUP AND PROCEDURE

The impedance tube was designed to use the two-microphone method described by Chung and Blaser[9] and in ASTM E 1050-90.[10] A standing wave field generated in the tube is measured by two microphones aligned along the length of the tube. The advantage of this method is that the absorption coefficient can be determined at multiple frequencies from a single measurement, as opposed to the standard probe-tube method,[11] which measures only one frequency at a time.

The impedance tube was designed to test a standard circular 4 in. diameter pavement sample. The inner diameter of the tube determined the cutoff frequency to be 1950 Hz. Measurements taken above cutoff are erroneous due to the presence of non-planar modes in the standing wave field. The impedance tube system is shown in Figure 3.1. The aluminum tube is 40 in. long and has a loudspeaker enclosed in a wooden box on one end, and a test sample holder on the other. Three possible microphone positions are located at 22, 30, and 35 cm (8.7, 11.8, 13.8 in.) from the test sample end of the tube. A 1/4 in. microphone is mounted in two of these locations, resulting in a microphone separation distance of 5, 8, or 13 cm (1.9, 3.1, 5.1 in.). The remaining mounting location is plugged. The test sample is placed in a short 4 in. tube with a 1.5 in. aluminum backing plate directly behind it. The short tube is held against the impedance tube with an outer aluminum sleeve.

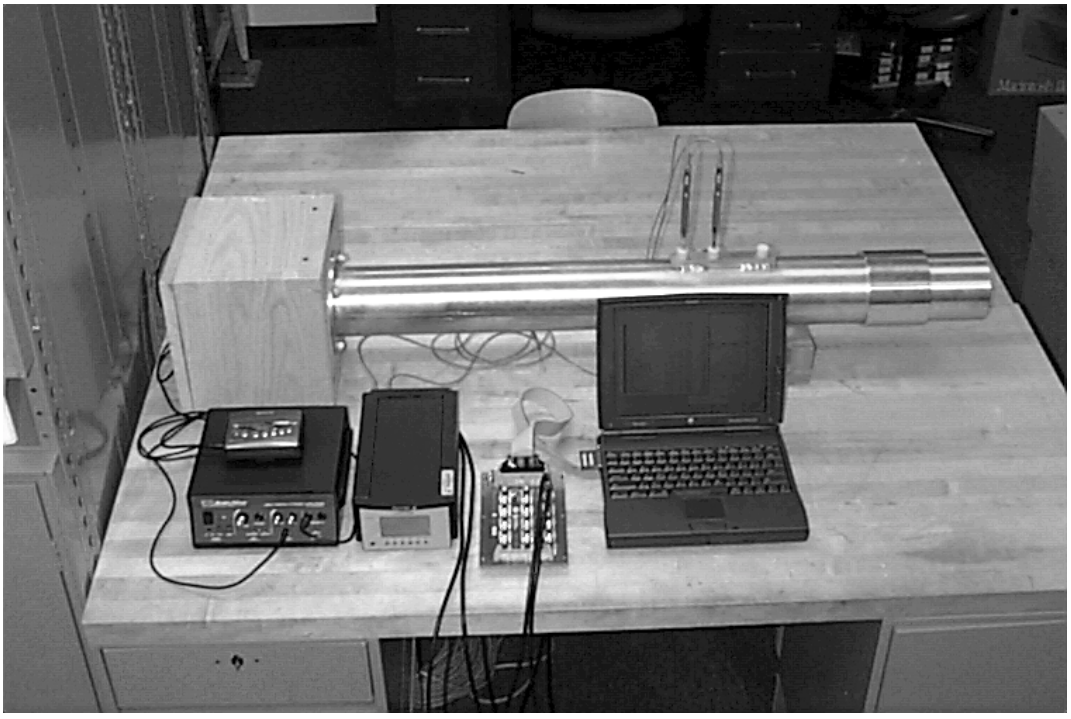

Figure 3.1. Impedance tube system.

During testing, prerecorded band-limited noise from 100 Hz to 2,000 Hz is amplified and sent to the loudspeaker. This creates the standing wave field in the tube between the driver and the test sample. The microphones measure the field at their respective locations. The time waveform signals from the two microphones are amplified to approximately 2 V peak-to-peak using a Brüel and Kjær Conditioning Preamplifier. The signals are also band filtered to reduce noise below 20 Hz and above 3,000 Hz.

The data collection is executed and processed by a laptop computer using Labview software. The amplified microphone signals are digitized at 20,000 samples per second using a National Instruments DAQ-1200 Card. Typically, the sample size is 4,096 points. The complex impedance and the acoustical absorption coefficient are displayed on the screen, and the data are saved in ASCI files.

Presented below are the equations used to solve for the acoustical absorption coefficient. A detailed derivation of the formulas can be found in the literature.[9,10] The pressure reflection coefficient R is calculated using the following:

$$R = \frac{H_{12} - e^{-jks}}{e^{+jks} - H_{12}}, \tag{3.1}$$

where *s* is the microphone separation distance, *k* is wave number, and H_{12} is a transfer function defined as

$$H_{12} = \frac{S_{12}}{S_{11}}. \qquad (3.2)$$

S_{12} is the cross-spectral density of the two microphones, and S_{11} is the auto-spectral density of the first microphone (see Fig. 3.2). During testing, a mean value of the transfer function is calculated by collecting multiple data sets. In addition, the two microphones are swapped halfway through the testing. A geometrical average of the swapped and unswapped transfer functions is calculated and then used to solve for the reflection coefficient. This error correction method, described by Chung and Blaser,[9] helps average out small differences in phase and sensitivity between the two microphones.

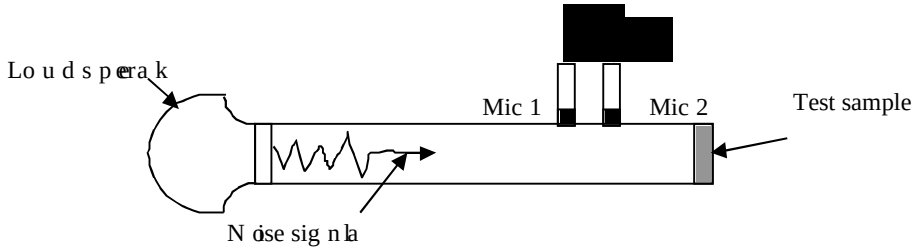

Figure 3.2. Diagram of impedance tube setup.

The absorption coefficient is given in terms of the reflection coefficient by $\alpha = 1 - |R|^2$. The process is typically repeated so that an average absorption coefficient can be calculated. Averaging multiple data sets helps smooth out any inconsistencies in the process.

3.2 CONSTRUCTION OF TEST SAMPLES

The first pavement samples were built and tested for parametric studies of varying thickness and aggregate size. These laboratory samples were not necessarily practical pavement designs in terms of strength or durability, but rather were manufactured to test the effect of specific parameters. Later, actual pavement design mixes were modified for testing. Aspects of their design mix, including aggregate size and percentage of screening, were varied to study the effect on the acoustical absorption. In addition to single-layer samples, double-layer samples were tested and modeled for noise absorption. The layers were chosen to represent realistic pavements, which normally consist of a relatively porous top layer over a denser bottom layer.

Samples were constructed at the TxDOT Superpave Laboratory in Austin. To accommodate the equipment dimensions, the pavement samples were constructed with a 4 in. diameter. Aggregate used in the samples came from stocks of limestone or siliceous river gravel stored at the facility. Test samples were made using standard laboratory hot-mix sample preparation techniques. Compaction was performed using a gyratory rotary

compactor. Standard dense ($\Omega<0.20$) samples were compacted to 3,500 psi. Porous samples ($\Omega>0.20$) were normally compacted to 1,500 psi.

The double-layer samples usually consisted of a very porous top layer and a denser lower layer. The goal in manufacturing these test samples was to simulate a core sample from a roadway consisting of two layers. However, it was difficult to achieve the proper compaction of the top layer without breaking or crushing aggregate in the lower layer. In those cases, the dense lower layer of hot-mix was compacted first and allowed to cool for approximately one hour. The lower layer was placed back into the mold and the material for the second layer was placed on top. The combined mixture was then placed in the rotary compactor. Compaction was modified from standard procedures because the lower layer was already compacted. Only a few cycles of rotary compaction were needed, regardless of the pressure sustained during the rotations of the sample. Following rotary compaction, the sample was compacted without rotation to 1,500 psi. Samples manufactured in this way tended to be slightly more compact than two layers that were compacted separately and then pressed together. It appeared that the top layer tended to enter into the lower layer during compaction, resulting in a slightly reduced thickness for the combined layer.

3.3 SINGLE-LAYER TEST RESULTS

Different parameters were studied in the single-layer tests in an attempt to determine which mixes yielded high absorption values. In the first series of tests, aggregate size and sample thickness were varied for comparison. Later tests were performed with actual pavement mixtures in which the percentage of smaller aggregate, called screening, was varied. An attempt was made to match some of the results to the existing theory for modeling a porous layer of pavement.

3.3.1 Effect of Thickness

A simple parametric study was conducted using very porous samples to determine the effects of thickness. Samples were constructed using only one size of aggregate and held together with 5 percent asphalt by weight. In decreasing aggregate size, specimens were made from C 1/2 in., C 3/8 in., F4, and F8 rock. Thickness sizes of 1 in., 2 in., and 3 in. were constructed for comparison. Figure 3.2 shows the results of the tests. The 2 in. sample for C 1/2 in. was broken before testing and therefore not included.

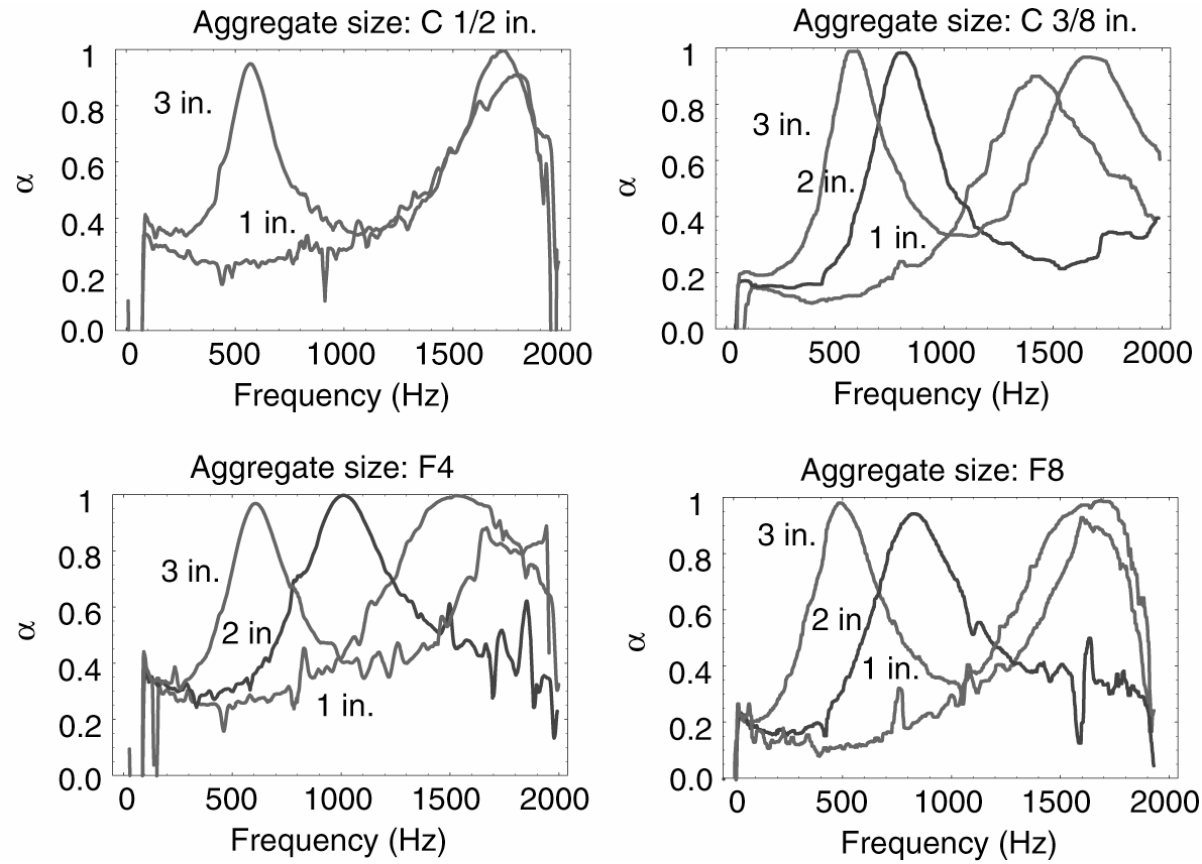

Figure 3.3. Absorption coefficient curve for four types of aggregate with varying thickness of 1 in., 2 in. or 3 in. The aggregate size decreases in order from C 1/2 in., C 3/8 in., F4 to F8.

The data show that all the samples have the distinct peaks in the absorption curves, as expected for a porous medium. The frequency of the lowest peak for a given aggregate size decreases with increasing thickness. With the 3 in. samples it is interesting to note the presence of a second peak for all four aggregate sizes.

3.3.2 Effect of Aggregate Size

The data set in Fig. 3.3 can be used to compare the effect of aggregate size. Figure 3.4 below shows the results of that comparison.

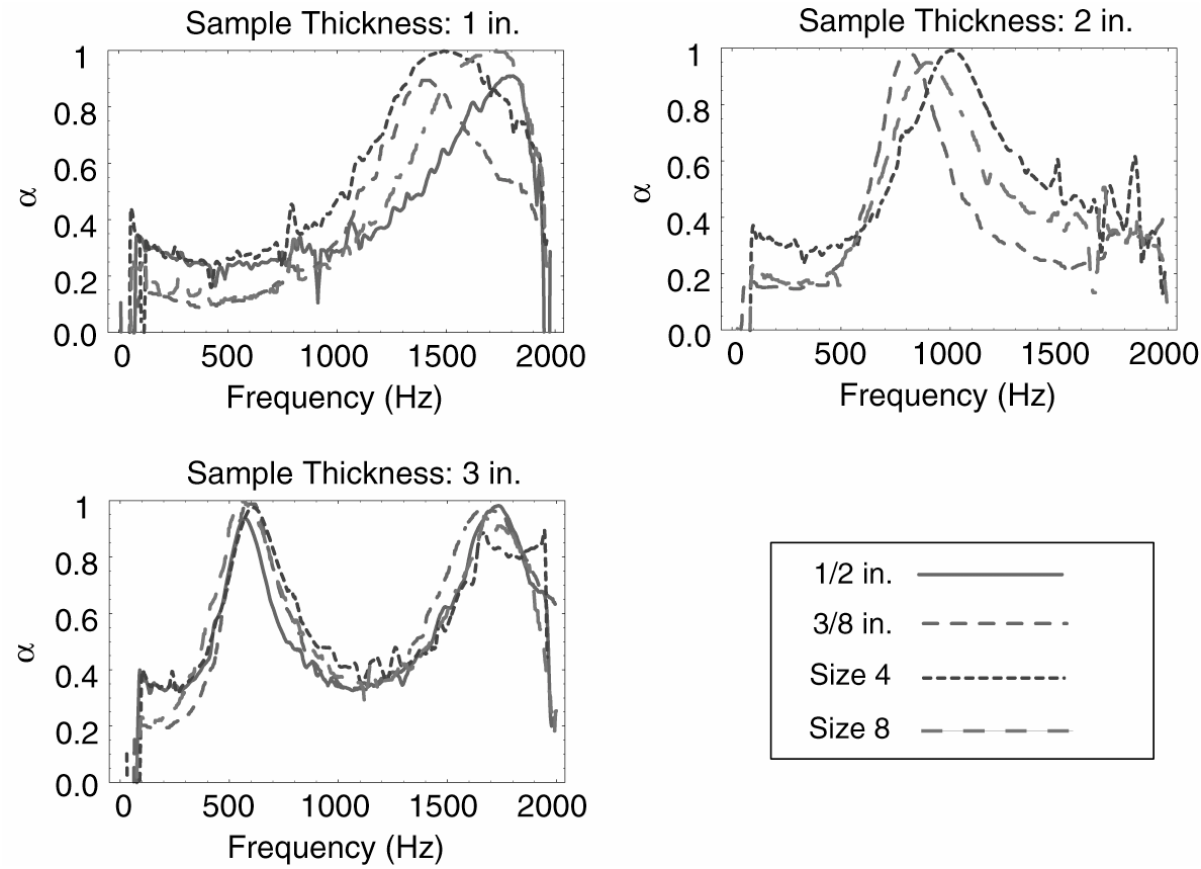

Figure 3.4. Three graphs showing absorption coefficient curves for 1 in., 2 in. and 3 in. samples compared with respect to aggregate size.

The peak frequency of the absorption curve is determined by the sample thickness ℓ and shape factor *K*. For these samples, ℓ remained relatively constant, and thus small shifts in frequency are likely due to slight differences in *K*. However, changing the size of the aggregate appears to have a small effect on the measured absorption.

3.3.3 Effect of Variation in the Percentage of Screening

Two commercial pavement designs, called NovaChip and New Jersey Mix, were chosen to study the effect of changing the percentage of small aggregate content on the measured absorption coefficient. Porosity Ω was also measured for the purpose of comparison. The modified mixes had less small aggregate than the unmodified mixes. The goal was to increase Ω by decreasing the ratio of small aggregate to large aggregate. Each sample was made using exactly 500 g (1.10 lbs.) of aggregate composed primarily of 3/8 in. and size 4 rock. In Appendix A, the exact composition of each specimen is listed in their corresponding batching sheets. A standard method for measuring the specific gravity of the

aggregate and asphalt mixture was implemented at the TxDOT Pavement Facility. Ω was determined after weighing and measuring the volume of each test sample.

Samples are constructed by mixing the aggregate in several batches, called bins. Aggregate size and amount are specified in each bin according to percentage of total weight. The original NovaChip mix was modified by replacing a percentage of its screening contained in bin 2 with mostly size 4 rock from bin 1. A small amount of very fine aggregate was left in the mix so that the asphalt would still bond to the rocks. Table 3.1 lists the porosity and thickness for the original and modified mixes used in the study. Since the original NovaChip contained a fair amount of screening, the modified mixes had a significantly higher porosity than the original mix. This also may have been the reason for the increase in thickness.

TABLE 3.1. *Measured thickness and porosity of test specimens.*

SAMPLE NAME	Thickness (in.)	Ω
NovaChip 23% Screening (original mix)	1.23	0.140
NOVACHIP 11.5% SCREENING	1.30	0.190
NovaChip 0% Screening	1.40	0.245
New Jersey 40% Bin 2 (original mix)	1.25	0.258
New Jersey 20% Bin 2	1.25	0.226
New Jersey 0% Bin 2	1.25	0.256

Unlike for NovaChip, the screening for the New Jersey mix was not batched as a separate bin. However, most of the smaller aggregate was contained in bin 2. Reducing the percentage of bin 2 reduced the amount of size 8 aggregate and replaced it with mostly size 4 aggregate from bin 3. The original design calls for 40 percent of the aggregate by weight to be from bin 2. Thus, the sample called New Jersey 20 percent bin 2 is 20 percent of bin 2 by weight, and 20 percent of bin 3. The remaining 60 percent of the aggregate is the same as the original mix. See Appendix A for specific batching details. The results of the absorption tests are presented in Figure 3.5.

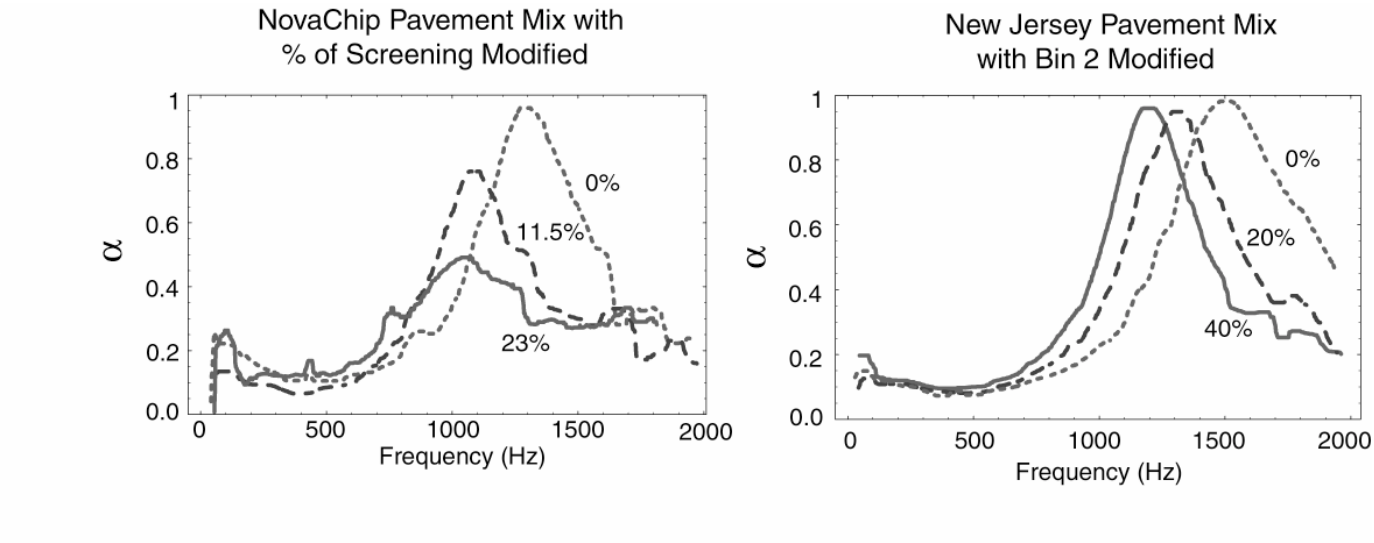

Figure 3.5. Two graphs showing the absorption coefficient curves for the two pavement design mixes, NovaChip and New Jersey, with two modified mixes for each.

The data from the NovaChip tests suggest that reducing the screening increased the overall absorption peak of the specimen. The frequency of the peak absorption also increased. On the other hand, the screening of the New Jersey was already low. Therefore, replacing bin 2 with more size 4 aggregate changed Ω and the overall absorption only slightly. The increase in frequency of the absorption peaks for both modified designs is likely due to a decrease in K.

Predictions using Eq. (2.13) show that Ω determines the amplitude of the absorption peak. The data is consistent with this theory when comparing the similarity of the absorption curves of the NovaChip 0 percent screening and the New Jersey 40 percent bin 2, since they both have a $\Omega \approx 0.25$. The data suggest that using a more uniform aggregate mix slightly increases the overall absorption. Unfortunately, realistic pavements cannot be constructed entirely of one aggregate size, due to strength and asphalt bonding concerns. Thus a physical limit on the absorption has likely been reached with the New Jersey and modified NovaChip designs.

3.3.4. Matching Porous Media Theory to Data

It is possible using Eq. (2.13) to predict the absorption curve of a pavement sample if the thickness ℓ, porosity Ω, air resistivity R_S, and shape factor K are known. With the exception of K these quantities can be measured using standard laboratory techniques. The shape factor only effects the location of the frequency of the peaks in the absorption curves; therefore, the theory can be matched to the data to find K. Berengier et al.[2] found good agreement between predicted and measured values of absorption.

In our study, only Ω and ℓ were measured. However, a prediction of R_S and K can be made by curve fitting the theoretical prediction to the measured data. An example case of a

1 in. sample made solely of aggregate size 8 bound together with 5 percent asphalt cement is shown in Figure 3.6. The sample porosity Ω was 0.38. This example found R_S = 40,000 N s/m^4 and K = 3.5.

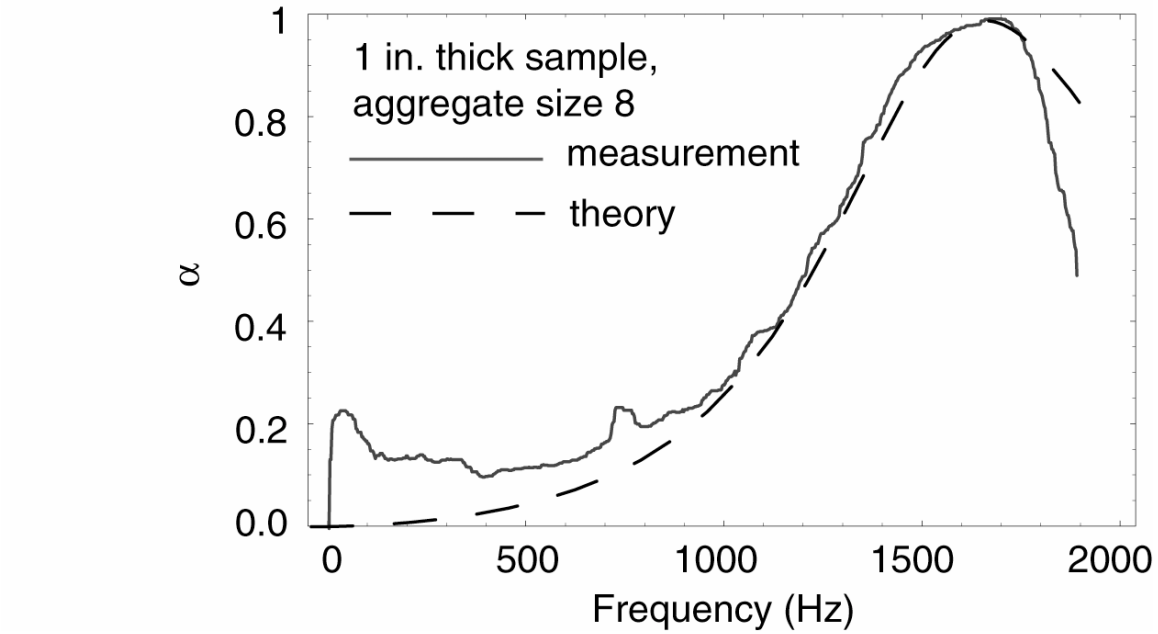

Figure 3.6. Theory and experimental results of the absorption coefficient in the frequency span of 100 to 1,900 Hz for a 1 in. thick sample of aggregate size 8.

The theory matches the experiment well for $\alpha > 0.2$. The measurements in the frequency range of 0-500 Hz are probably inaccurate due to the low absorption of the sample and the limits of the test apparatus to measure low values of absorption. Likewise, there is also a limit to the accuracy of the impedance tube at higher frequencies approaching the 1950 Hz cutoff. The ability to predict absorption of typical samples will prove useful when we attempt to optimize pavement design for low noise, especially when constructing pavement with more than one layer.

3.4 DOUBLE-LAYER RESULTS

Since real road surfaces are often constructed in layers, a few double-layer samples were constructed and analyzed. Using the preceding method for matching theoretical curves to measured absorption curves, it is possible to use Eqs. (2.16)-(2.22) to predict α for a double-layer sample. First, two single-layer samples were constructed and measured in the impedance tube. The theory was matched to the measurements to obtain R_S and K. With Ω and K determined, the theory was applied to predict an absorption curve for a double layer. An actual specimen was then constructed and measured. Figure 3.7 shows the results for the single-layer and double-layer absorption curves for a more porous top layer pavement

(Ω=0.254) and a more dense bottom layer pavement (Ω=0.10). The experimental data plotted with the theoretical model prediction show that the theory is reasonably accurate for the double-layer sample. Table 3.2 lists the parameter values used to generate the graphs.

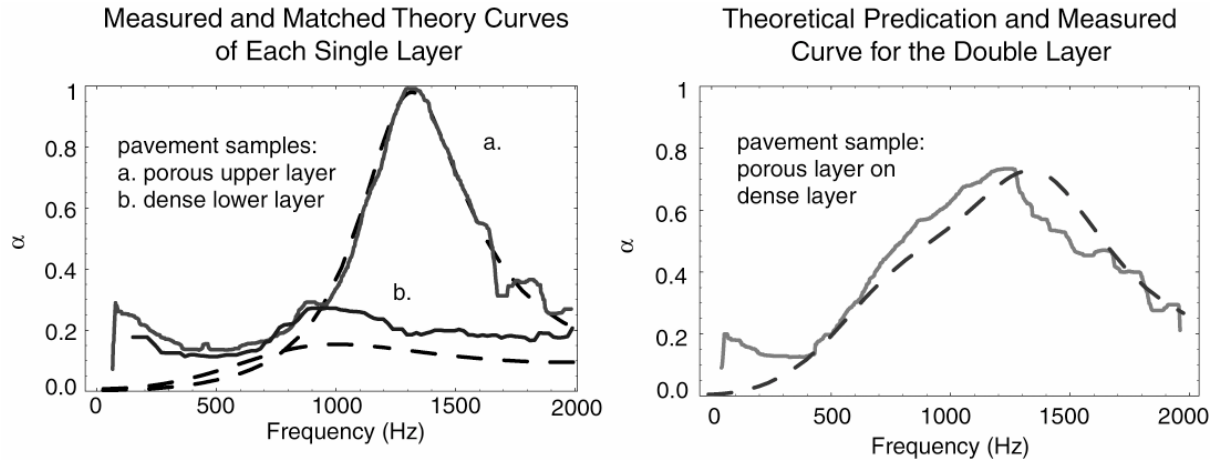

Figure 3.7. Graphs showing absorption coefficient curves for a porous upper and dense lower layer. Curves shown are for each layer separately and for the combined sample. Dashed lines are theory; solid lines are experimental results.

TABLE 3.2. *Parameter values used to predict the theory for Figure 3.7.*

Parameter	Top-layer NovaChip with 0% screening	Dense Bottom-layer Pavement
ℓ	1.4 in.	1.2 in.
Ω	0.254	0.10
R_S	38,000 N-s/m^4	750,000 N-s/m^4
K	3.7	8

The double-layer absorption shown in Figure 3.7 has a lower maximum value but a broader peak, and in particular, higher absorption from 500 to 1,100 Hz. Because traffic noise typically is broadband with highest energy levels between 800 Hz and 1,000 Hz, the double-layer sample may actually perform better than the single-layer sample.

Another double-layer sample was made and tested using a semi-dense bottom layer (Ω=0.16). These results are shown in Figure 3.8. Both examples show that the absorption curve of the porous sample changes significantly when backed by another sample, even when that sample is relatively dense. If the density of the lower layer is increased, the overall absorption curve moves closer to the results for the upper layer alone. For the second case, the absorption curve has two peaks, one near 700 Hz and one near 1,400 Hz. Compared to the other double-layer sample, the latter sample has higher absorption in the low frequency range but lower absorption near 1,000 Hz. Since traffic noise has its highest energy levels around 1,000 Hz, this second double-layer sample, although more porous than the first, may not be as effective at noise reduction.

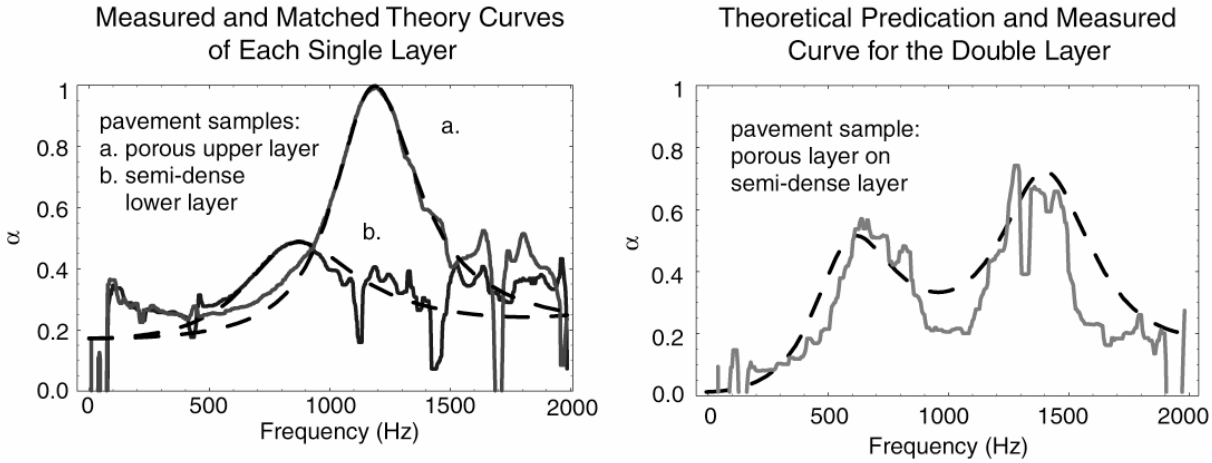

Figure 3.8. Graphs showing absorption coefficient curves for a porous upper and semi-porous lower layer. Curves shown are for each layer separately and for the combined sample. Dashed lines are theory; solid lines are experimental results.

TABLE 3.2. *Parameter values used to predict the theory for Figure 3.8.*

Parameter	Top Layer New Jersey Mix	Semi-Dense Bottom Layer
ℓ	1.25 in.	1.26 in.
Ω	0.258	0.159
R_S	37,000 N-s/m^4	230,000 N-s/m^4
K	3.7	9.2

CHAPTER 4 . REVERBERATION ROOM TESTS AND RESULTS

Another standardized technique for measuring acoustical absorption is the reverberation room method. The noise reduction coefficient (NRC) rating used by industry to specify building materials and acoustical products is calculated using this method. The current standard is designated as ASTM C 423–90a.[12] Unlike the impedance tube method, the reverberation room method measures the absorption of sound in a diffuse field, meaning sound waves strike the test sample at random angles of incidence. Since real-world conditions are diffuse, the reverberation room method may be a more accurate model for testing acoustical absorption of pavement. However, the method tends to over-predict acoustical absorption due to the diffraction effect.[12]

Explained below is the test setup and procedure used for this study. The reverberation standard[12] requires that the test sample area is at least 48 ft^2, and therefore a particularly large section of pavement was needed. A description of the test sample and its construction is included. Owing to time and cost considerations, only one pavement type was tested using this method. However, some insight may be gained into the noise absorption properties of pavement through this example. The chapter concludes with the test results and a discussion of the differences between the impedance tube and reverberation room methods.

4.1 TEST SETUP AND PROCEDURE

Tests were conducted in the reverberation room chamber located in the Engineering Science Building at the University of Texas at Austin. The chamber measures 29 by 19 by 16 ft 8 in. (l × w × h) and maintains a relatively constant 60 percent relative humidity and 73 ^{O}F temperature.[13] It is built into the ground so that the ceiling is even with the foundation of the basement level. The floor and walls are concrete construction, and a wooden commercial lay-in ceiling has been placed over the chamber. The chamber is entered from above by descending a ladder through a small hatch in the floor of the basement.

To measure acoustical absorption of a test sample, a decay time must be measured for both the empty chamber and the chamber containing the sample. Decay time, typically referred to as T_{60}, is defined as the time in seconds it takes the sound pressure level (SPL) of a noise signal to decay 60 dB inside a given space. The Sabine equation taken from a standard reference[14] approximates the decay time in terms of the room dimensions and the absorption coefficient values of all the exposed surfaces:

$$T_{60} = \frac{0.049V}{\sum_i \alpha_i A_i}, \qquad (4.1)$$

where V is the volume of the room in ft^3 and $\sum_i \alpha_i A_i$ is the sum of all the exposed surface areas A_i in ft^2 multiplied by their corresponding acoustical absorption coefficients α_i. It follows that the equation for calculating the absorption coefficient for a test sample is

$$\alpha = \frac{0.049V}{A_S}\left(\frac{1}{T_{60\,full}} - \frac{1}{T_{60\,empty}} + \frac{A_S}{A_{Total}T_{60empty}}\right), \qquad (4.2)$$

where A_S is the area of the test sample in ft^2. Normally, the third term of Eq. (4.2) is neglected if $\frac{A_S}{A_{Total}} << 1$, i.e., if the surface of the sample occupies a small fraction of the surface of the chamber.

During testing, filtered pink noise was played through a loudspeaker located in one corner of the chamber. The loudspeaker was pointed towards the corner so as to excite more room modes. The pink noise was generated using a 1882 Random Noise Generator from General Radio Company, then one-third octave band filtered through a Brüel and Kjær Band Pass Filter Set Type 1612. A 1/2 in. microphone attached to a General Radio 1933 Precision Sound Level Meter was used to measure the sound pressure level (SPL). The microphone was located near a corner of the room, approximately 3 ft from any surface. A DC signal of the SPL was sent from the sound level meter to a Hewlett-Packard 54501A Digital Oscilloscope. The scope allowed the SPL to be captured as a function of time. The data from the scope were then acquired by a desktop computer using Hewlett-Packard Benchlink software. A diagram of the test setup is shown in Figure 4.1.

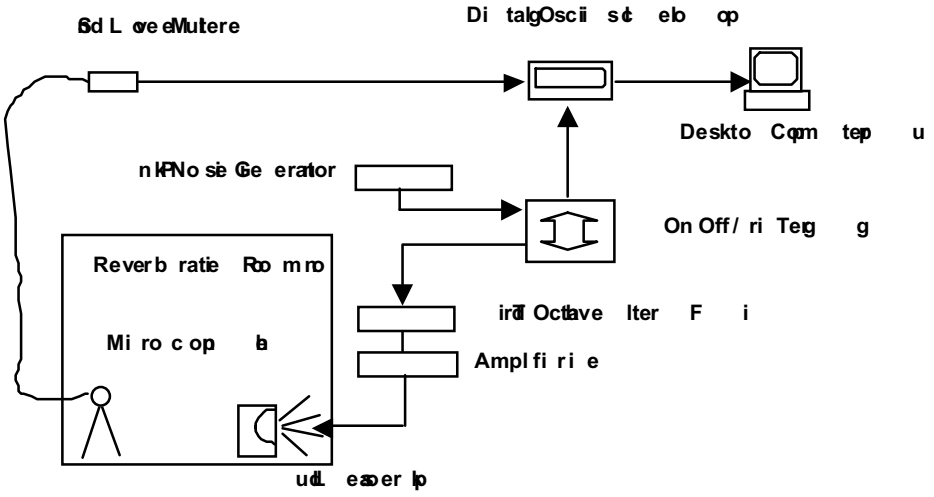

Figure 4.1. Diagram showing the test setup used for the reverberation room tests.

Tests began with the trigger on, allowing the pink noise to be sent to the loudspeaker. The noise was turned on for approximately 30 seconds to reach equilibrium, then turned off. At the moment of cutoff, the trigger device sends a signal to the oscilloscope, marking the start time of the decay. Data from the sound level meter were then collected until the SPL reached the noise floor. Each sample window contained 500 data points. Measurements were taken in one-third octave bands beginning at a center frequency of 125 Hz and

proceeding through 2,500 Hz. Fifty decay curves were collected and stored for each band. This procedure was followed for both the empty room and the room with the sample.

4.2 CONSTRUCTION OF TEST SAMPLE

The standard New Jersey design mix was chosen for the reverberation room study. The test sample was made up of sixteen 2 ft by 2 ft sections, for a total of 64 ft^2. The specimen was designed to have the same mass per unit area as a 500 g (1.1 lbs.), 4 in. diameter circular sample used in the impedance tube. Because of the odd size of this test sample, standard mixing and preparation methods could not be used in the manufacture of the test specimen. Samples were hand mixed and hand compacted in molds built from plywood and 2 in. by 4 in. lumber. All construction took place at the TxDOT Superpave Laboratory in Austin, Texas. Ten of the 16 sections were made using cold-mix asphalt. Cold-mix asphalt is an asphalt mixture containing a volatile emulsifier. The aggregate and asphalt mix is prepared cold and then allowed to sit. The pavement hardens as the emulsifier evaporates from the asphalt. The cold-mix was prepared in a wheelbarrow and poured into the molds and compacted. However, many of these specimens did not become sufficiently hard and had a tendency to crumble around the edges. The latter samples were made using a standard hot-mix. The hot-mix was prepared in several small batches since lab equipment was not available for the larger amounts. After the smaller batches were mixed, they were all poured into the sample mold and compacted. Owing to the unconventional construction of the pavement samples, there was some difficulty in making the entire specimen flat with a uniform thickness. An evaluation of the thickness is discussed below in the "Test Results" section of this chapter.

Upon completion, the sample was moved to the ENS building and lowered into the reverberation room section by section using a rope and pulley hoist. The plywood backing used in the molds was left intact so that the samples would not break apart in transit. The sixteen 2 ft by 2 ft pieces were arranged together in a large 8 ft by 8 ft section in the floor of the chamber as shown in Figure 4.2. The sample was placed slightly off center in the room as recommended by the standard.[12]

Figure 4.2. Photo showing test sample in reverberation room, with microphone in the background.

4.3 TEST RESULTS

Data were stored as text files and processed using MATLAB software. Figure 4.3 shows an example of a single decay curve recorded at 500 Hz for both the empty room and the room containing the sample. Cutoff of the signal to the loudspeaker begins at t=0 in each case. Since the data were recorded in volts per decibel, the graphs are referenced to an arbitrary dB level. Although it would be possible to calibrate the level in dB re 20 μPa, only the ratio of sound pressure level to noise floor is needed to calculate the absorption coefficient. The initial level was between 90 and 100 dB for most cases.

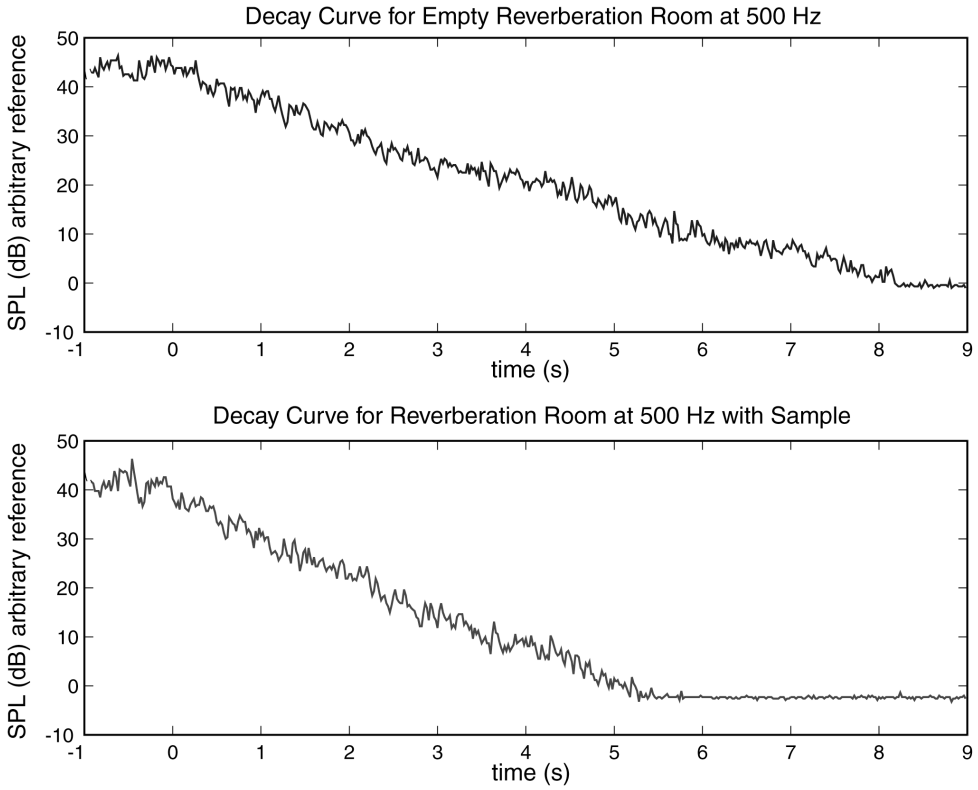

Figure 4.3. Graphs showing a single decay curve for the empty reverberation room and the room containing a sample for the 500Hz one-third octave band.

An absorption calculation begins by determining T_{60} for the empty room first and then doing so for the room with the sample. The current ASTM standard[12] contains no discussion or method for determining the T_{60} once a decay curve has been measured. Therefore, much of the data analysis procedure was followed under the advisement of David Nelson,[15] formerly of Acoustic Systems in Austin, Texas. A common method for calculating T_{60} is to perform a linear regression on the data to find the slope of the decay curve. Linear regression is a common statistical technique that uses a set of data points $(\overline{X}, \overline{Y})$ to solve for the coefficients of the equation

$$\overline{Y} = b\overline{X} + c\,. \tag{4.3}$$

The slope *b* in terms of dB per second is used to calculate T_{60}. Formulas for calculating the coefficients and subsequent statistical operations, including standard deviation, can be found in a standard reference text.[16]

A consistent method was implemented when choosing the part of the slope to use for the linear regression.[15] Data points were taken beginning at 100 ms after cutoff until the signal level dropped 25 dB. All fifty trials were included in the data set used to calculate the linear fit for each test case. The value of T_{60} and its standard deviation were then calculated.

In all cases, the standard deviation was small, indicating that the data sets were very consistent.

An example of the 500 Hz data is shown in Figure 4.4. The graph shows the data points from all fifty runs for each test case. The line fits based on Eq. (4.3) are shown with a –15 dB offset to separate them from the data for clarity. The horizontal extent of each line corresponds to the time interval over which the average was performed for that case. The remaining graphs for each third-octave band are presented in Appendix B.

Figure 4.4. Graphs showing all fifty decay curves for the empty room and room with pavement samples at 500 Hz. Included is the line fit (15dB down), shown as the black line, and decay time in seconds with its standard deviation.

Listed in Table 4.1 are the decay times and absorption values found at all 14 frequency bands considered. The data show that the peak absorption of the pavement sample is in the 1,600 Hz band. In addition, the reverberation chamber exhibits a decreasing trend in decay time from low to high frequency. This room characteristic was also found in the study done by Irrgang.[13] One exception is the increase in reverberation time from 160 Hz to 200 Hz. For these low frequencies, some of the sound energy may be transmitted through the concrete walls and wooden ceiling, resulting in shorter decay times.

TABLE 4.1. *Values of T_{60} for each third-octave band used to calculate the acoustical absorption of the test sample.*

1/3 Octave Band (Hz)	T_{60} for Empty Room (sec)	T_{60} for Room with Sample (sec)	Acoustical Absorption α
125	12.54	11.76	0.050
160	11.31	10.51	0.061
200	17.89	16.92	0.032
250	13.11	12.62	0.034
315	11.65	9.63	0.141
400	11.02	8.57	0.197
500	10.91	7.57	0.300
630	9.26	5.97	0.439
800	6.93	4.55	0.555
1000	6.43	4.29	0.570
1250	5.19	3.59	0.636
1600	4.47	3.20	0.662
2000	4.02	3.03	0.615
2500	3.35	2.73	0.523

For the purpose of comparison, six core samples 4 in. in diameter were randomly cut out of different sections of the test specimen. The core samples were measured for thickness then tested in the impedance tube. The two methods for determining acoustical absorption measure two uniquely different test conditions; therefore, some differences in the predicted values are expected. The purpose of this study is not to compare the two methods explicitly, but to gain some insight into the absorption properties of porous asphalt by using both types of tests. The impedance tube absorption data from the core samples were put into one-third octave bands to compare to the reverberation room predictions. The graph in Figure 4.5 shows the comparison of these data. The core samples had absorption curves very similar to the New Jersey specimens tested in Chapter 3 (Fig. 3.5). Their peak absorption frequency varied between 800 Hz and 1000 Hz and approached $\alpha = 1.0$ near the top of the curve. In contrast, the reverberation data in Figure 4.5 show a steady increase in absorption and do not show the same peak values in the given frequency range.

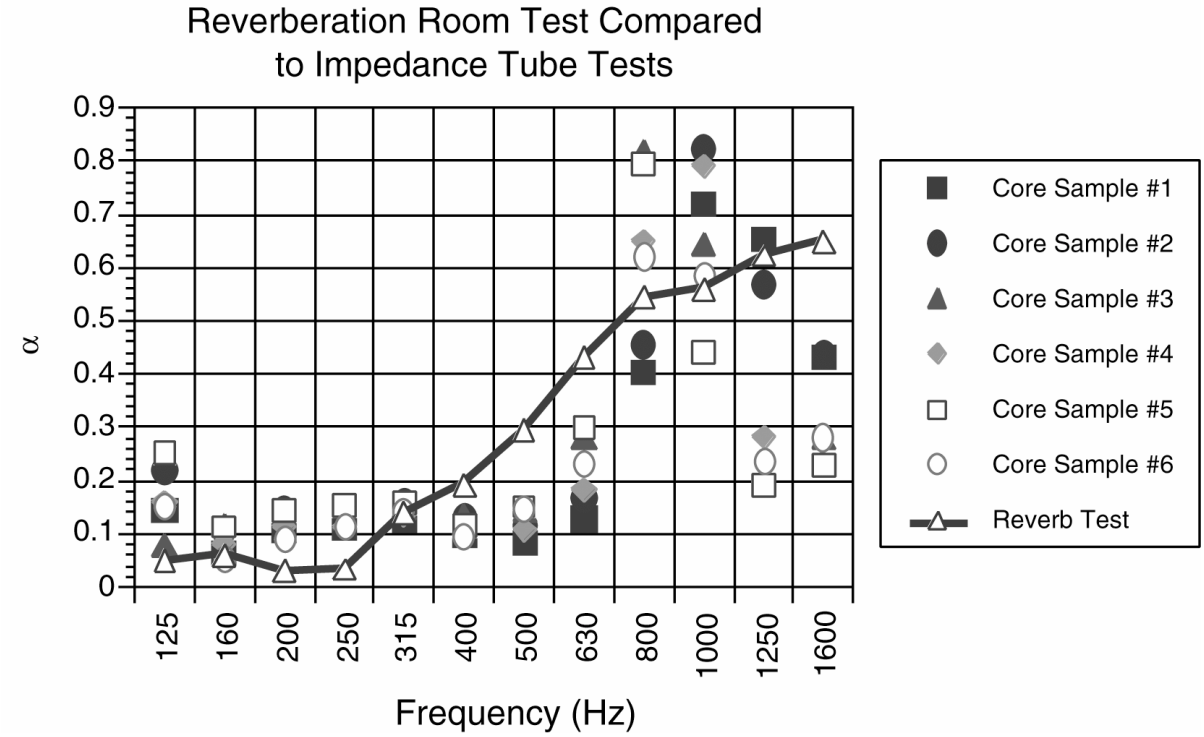

Figure 4.5. Graph comparing absorption coefficient data in one-third octave frequency bands for the reverberation tests and the six core samples tested in the impedance tube.

One possible explanation in the difference between the two methods is the variation in thickness of the core samples. From the previous single layer impedance tube studies, small variation in the thickness may shift the frequency of the peak absorption. Table 4.2 lists the core samples and their respective thickness. A measurement survey of the large test specimen indicated that its thickness ranged from 1.19 in. to 1.67 in. Although a small sample size was used, a straight average of the values of α of the core samples was calculated and compared to the reverberation room tests in Figure 4.6. Based on the findings in Section 3.3.1, the variation in thickness of the large test sample should cause a flattening in the absorption peak.

TABLE 4.2. *Core sample thickness data.*

Core Sample #	Thickness (in)
1	1.21
2	1.29
3	1.52

4	**1.50**
5	**1.40**
6	**1.44**

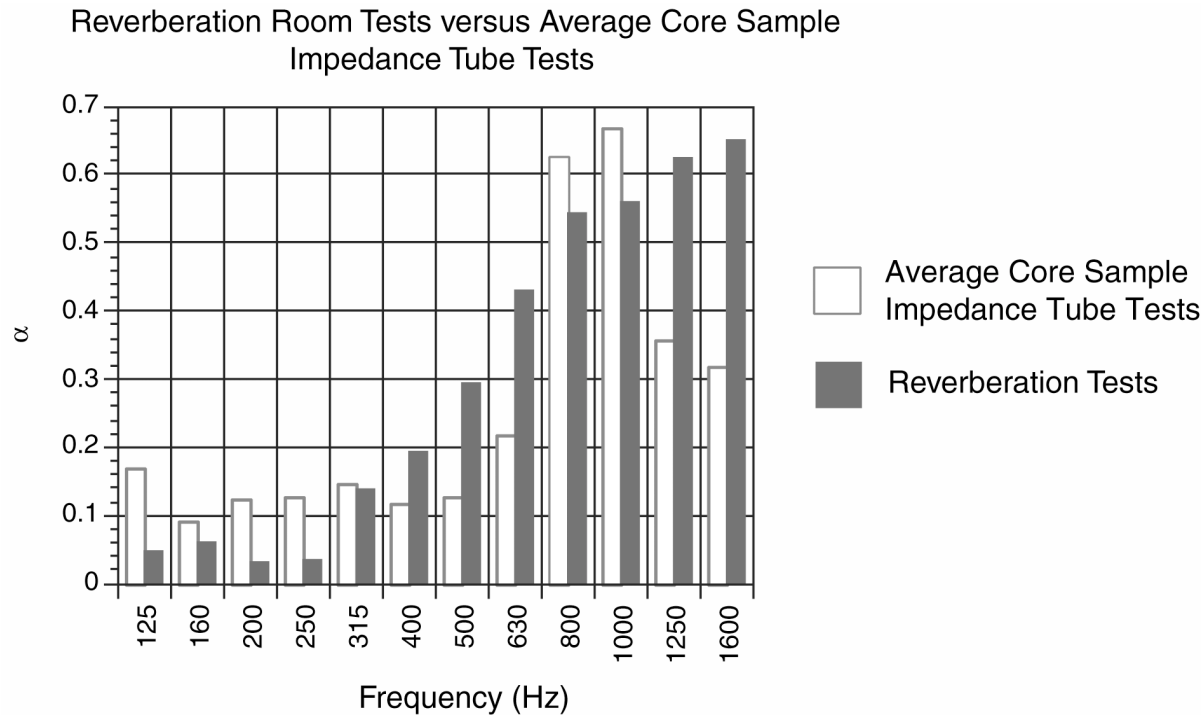

Figure 4.6. Graph comparing reverberation room tests to the average impedance tube measurements of all six core samples.

Comparison of the two methods shows a distinct difference in the absorption trend for the 1,250 Hz and 1,600 Hz one-third octave bands. Although averaging the impedance tube measurements flattens out the absorption peak somewhat, there is clearly some discrepancy between the two methods. Previous studies have shown that the reverberation room method tends to over predict absorption because of diffraction effects.[17] These effects may have been exaggerated in the 1,250 Hz and 1,600 Hz reverberation room tests. In any case, it may be inferred that noise reduction predictions for porous pavement based on normal incidence theory[2] may differ with actual measured roadside data.

CHAPTER 5 . IMPLICATIONS FOR QUIET PAVEMENTS

This section begins with a review of previous research on tire/road noise followed by a description of how the double-layer theory explained in Chapter 3 is applied to porous asphalt design. The next section includes an estimate of the noise reduction attained by using porous asphalt pavement. The chapter ends with conclusions and recommendations for future work.

5.1 DESCRIPTION OF TIRE/ROAD NOISE

The data[1,3,4] have shown that using porous asphalt decreases measured roadside noise by as much as 6 dB over traditional pavements. However, the thickness of commercial porous overlays tends to be less than 1 in. This means the absorption peaks of these overlays are well above the 800 Hz to 1,000 Hz range where road noise is most prominent. A straightforward calculation of noise reduction, as explained in Section 5.2, predicts no significant decrease in noise level using thin porous overlays. This suggests that current porous asphalt roads are not achieving noise reduction from direct absorption only. Additional reflections from sound waves bouncing between the vehicle and the pavement may account for the lower noise levels. The other significant factor is the decrease in noise generation.

There has been a considerable amount of research done on the mechanisms of tire/road noise generation. Although there remains some controversy as to the importance of each mechanism, the following phenomena, compiled by Sandberg,[18] are all considered sources of noise generation.

- Radial vibration mechanism – impact of tire tread on road surface and vice versa.
- Air resonant mechanism – pipe resonance, Helmholtz resonance, and pocket air-pumping, associated with the expansion/compression of entrapped air in the tire treads and road surface.
- Adhesion mechanism – stick/slip motions caused by tangential tire vibrations and rubber-to-road stick/release effect.

In addition, further investigation has shown that other phenomena influencing noise amplitude include the horn effect, sound absorption in the road surface, and mechanical impedance of the road (pavement stiffness).

The properties of porous pavements likely reduce the mechanisms of air resonance and adhesion. We have hypothesized that porous asphalt may decrease the noise generation from the air resonance mechanism by reducing the effect of trapped air pockets between the tire and road surface. Mentioned in Chapter 1 are the experiments done by Iwai et al.[5] that showed the influence of porous asphalt pavement on the horn amplification of tire/road noise. The researchers showed that less noise was generated near the pavement surface for porous asphalt. The conclusion is that a decrease in noise generation as well as the acoustical absorption properties may be responsible for the measured noise reduction of porous asphalt. Since many current porous pavement designs are not optimized for acoustical absorption

performance, it may be possible to achieve much greater noise reduction by tuning the absorption peak of the porous layer to the traffic noise spectrum.

5.2 PAVEMENT DESIGN FOR REDUCED TRAFFIC NOISE

It was shown in Chapter 3.4 that acoustical absorption α can be predicted for a double-layer pavement sample using Eqs. (2.16-2.22). α is calculated from four physical parameters for each pavement layer. Given Ω, R_s, and K, the thickness e may be varied to optimize α. These parameters can be determined by curve fitting the measured data for single layer samples to the theoretical predictions found using Eq. (2.13). A practical design problem might be to design the thickness of a top porous layer to be laid on top of a dense existing pavement layer.

For this example, data from an actual road noise spectrum were used to optimize the noise reduction gained from acoustical absorption. Figure 5.1 shows the one-third octave spectrum for road noise gathered by the Center for Transportation Research for a study funded by the Texas Department of Transportation (TxDOT).[3] The data were measured from a new asphalt surface. Stationary microphones recorded the noise generated from a passing test vehicle.

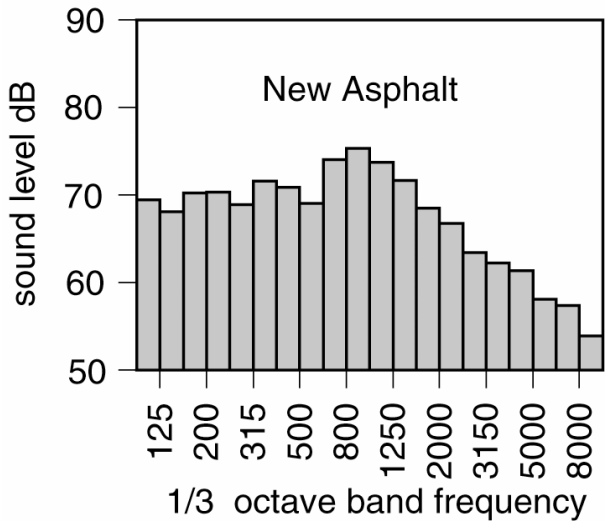

Figure 5.1. Graph showing measured noise spectrum recorded next to a new asphalt surface during roadside tests.

We concluded in Chapter 3 that the New Jersey and modified NovaChip designs achieved the maximum amount of acoustical absorption attainable using realistic pavement mixtures. Therefore, the modified NovaChip design with 4 percent screening was chosen as the porous overlay surface for the example pavement design. Assuming a 3 in. thick dense (5 percent void) pavement for the bottom layer, Eqs. (2.16-2.22) were used to try and match the predicted absorption to the noise spectrum of the new asphalt surface. The thickness of the NovaChip layer was optimized to achieve a peak absorption near 1,000 Hz, where the

new asphalt noise spectrum is greatest. Figure 5.2 shows the predicted values of α as a function of frequency. Below in Table 5.1 are the values of the parameters used to generate the graphs. The parameters other than thickness were determined by matching actual absorption curves to theory as explained in Section 3.4.

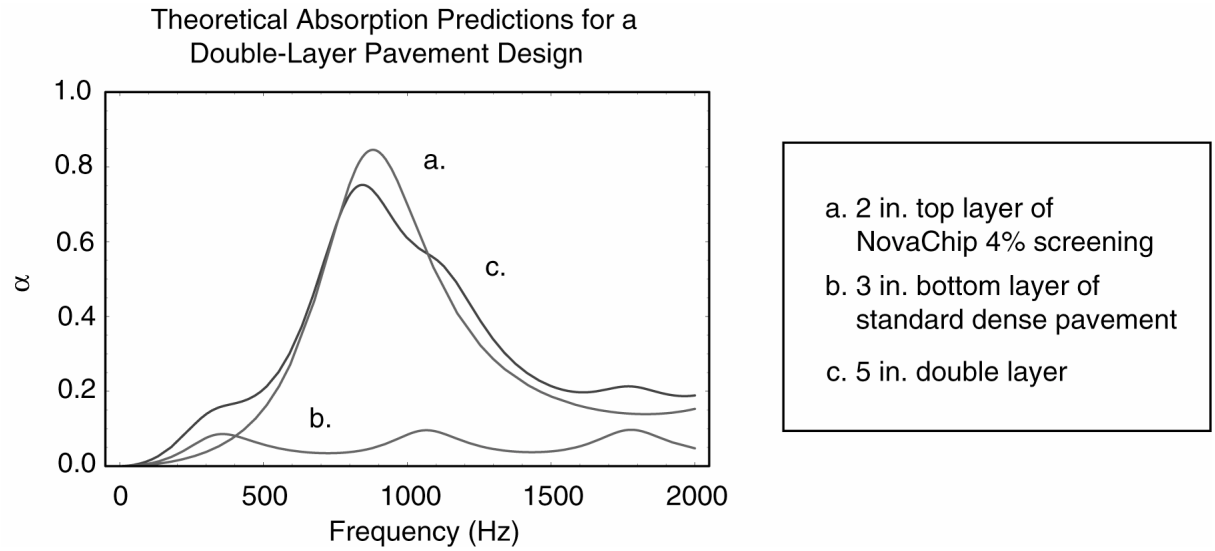

Figure 5.2. Graph showing theoretical absorption predictions for a double-layer pavement with a NovaChip modified design top layer on top of a dense pavement.

TABLE 5.1. *Physical parameters used for double-layer pavement design.*

Parameter	Top-layer NovaChip with 4% screening	Dense Bottom-layer Pavement
ℓ	1.75 in.	3 in.
Ω	0.254	0.05
R_S	38000 N-s/m^4	500000 N-s/m^4
K	3.7	11

Figure 5.2 shows that the peak of the absorption curve falls around 1,000 Hz, close to the peak of the noise spectrum data in Figure 5.1. A prediction of the noise reduction can be made by assuming all acoustical absorption is achieved directly at the noise source. Thus, additional absorption from reflections off the pavement surfaces is not considered. All other sources of acoustical absorption are also assumed constant, including losses due to spreading and decreases in sound generation. Figure 5.3 shows the roadside noise measured from new asphalt compared to the predicted roadside noise using a porous asphalt overlay. We see a decrease in the 1,000 Hz band of nearly 6 dB. Although this may account for only 2 dB in overall noise reduction, the perceived noise reduction will be much greater by eliminating the tonal aspect of the noise spectrum. The porous layer also attenuates the peak energy in the frequency range where humans are most sensitive. Considering other noise reduction factors

such as decreased noise generation and multiple reflections off the pavement surface, we predict a decrease in roadside noise levels of 8 dB or higher using this example pavement design.

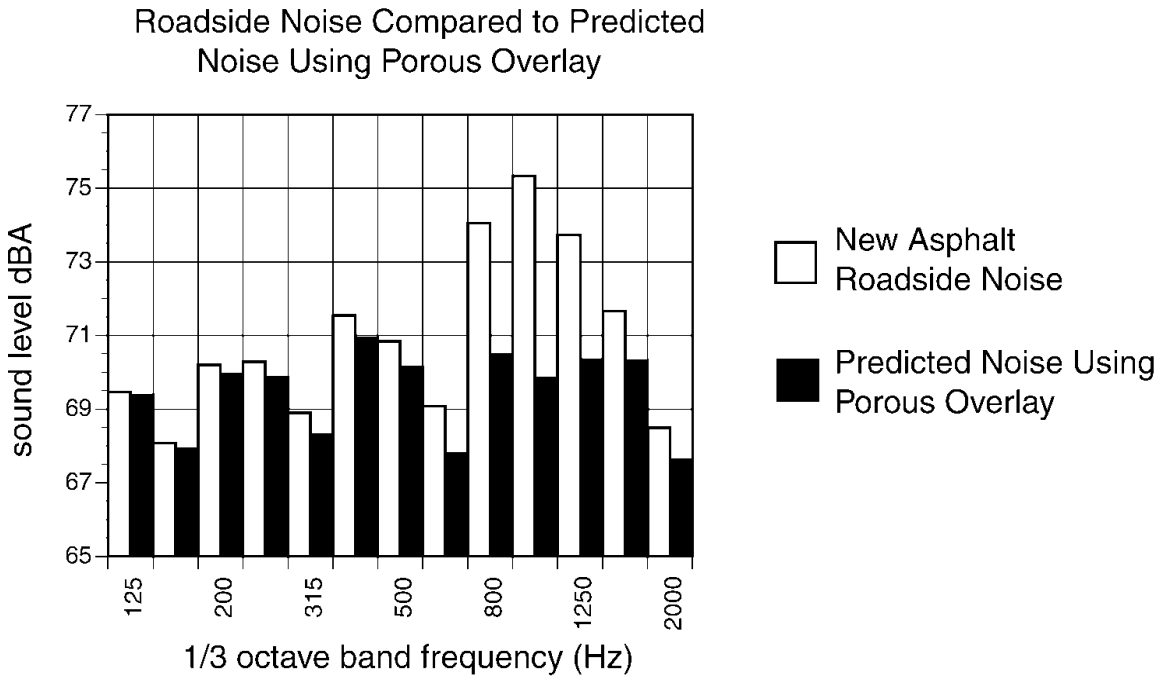

Figure 5.3. Graph showing actual roadside noise tested using new asphalt compared to predicted roadside noise using porous overlay.

5.3 CONCLUSIONS AND RECOMMENDATIONS FOR FUTURE WORK

It should be repeated that the predicted acoustical absorption described in Chapter 3 applies to sound waves striking the pavement at normal incidence. Although noise is generated at the tire/pavement interface,[5] there are many transmission paths the noise may take to a receiver. The authors conclude that an accurate prediction of noise reduction cannot be made solely based on acoustical absorption. Other factors, including multiple sound wave reflections off the pavement surface and the decrease of noise generation, also affect the acoustical performance of porous pavements. It therefore becomes necessary to test real pavement surfaces to determine how important acoustical absorption is in determining the measured noise reduction of porous pavements. A survey of actual pavement surfaces that correlates measured tire noise to acoustical absorption could offer some insight into how absorption can be used to predict noise reduction for porous asphalt. This might also resolve some of the discrepancies found between the diffuse-field and normal-incidence absorption measurements.

The current impedance tube setup was designed to be portable so that actual pavement roads could be acoustically tested on site. The tube stand shown in Figure 5.4 was

built to facilitate the measurement of flat surfaces. All of the equipment to run the impedance tube system is battery powered to allow for easy transportation and data collection. A small test section of absorptive pavement could be designed and constructed to have improved performance between 800 Hz and 1,000 Hz. Comparing absorption data and tire noise data gathered on the test section would assist development of a method for estimating noise reduction in SPL.

Figure 5.4. Impedance tube with stand for measuring acoustical absorption of flat surfaces.

APPENDIX A. BATCHING INFORMATION FOR SELECTED PAVEMENT MIXES

TABLE A.1. *Batching sheet for standard NovaChip.*

Sieves		Materials (% Passing)		
US UNITS	SI	BIN 1	BIN 2	BIN 3
1	25	100.0	100.0	100.0
7/8	22.4	100.0	100.0	100.0
1/2	12.5	100.0	100.0	100.0
3/8	9.5	93.5	100.0	100.0
No. 4	4.75	3.5	100.0	100.0
No. 10	2	0.7	93.0	100.0
No. 40	0.425	0.6	28.8	100.0
No. 80	0.18	0.5	8.7	100.0
No. 200	0.075	0.3	3.5	100.0
Pan	Pan	0.0	0.0	0.0

TABLE A.2. *Bin percentage used for standard NovaChip 23% screening.*

COMPONENT	% Blend by Weight
BIN 1	73
BIN 2	23
BIN 3	4

TABLE A.3. *Bin percentage used for modified NovaChip 11.5% screening.*

COMPONENT	% Blend by Weight
BIN 1	84.5
BIN 2	11.5
BIN 3	4

TABLE A.4. *Bin percentage used for modified NovaChip 0% screening.*

COMPONENT	% Blend by Weight
BIN 1	96
BIN 2	0
BIN 3	4

TABLE A.5. *Batching sheet for standard New Jersey.*

Sieves	Materials (% Passing)

US UNITS	SI	BIN 1	BIN 2	BIN 3	FILLER
3/4	19	100.0	100.0	100.0	100.0
1/2	12.5	100.0	100.0	100.0	100.0
3/8	9.5	100.0	100.0	82.9	100.0
No. 4	4.75	97.2	39.1	4.1	100.0
No. 8	2.36	89.8	4.1	2.0	100.0
No. 16	1.18	74.0	3.2	1.5	100.0
No. 30	0.6	46.3	2.5	0.9	100.0
No. 50	0.3	15.4	1.1	0.6	99.7
No. 100	0.15	2.0	0.7	0.5	97.8
No. 200	0.075	0.6	0.6	0.4	87.7
Pan	Pan	0.0	0.0	0.0	0.0

TABLE A.6. *Bin percentage used for standard New Jersey (40% bin 2).*

COMPONENT	% Blend by Weight
BIN 1	**2.8**
BIN 2	**40.1**
BIN 3	**53.3**
FILLER	**3.8**

TABLE A.7. *Bin percentage used for modified New Jersey (20% bin 2).*

COMPONENT	% Blend by Weight
BIN 1	**2.8**
BIN 2	**20.05**
BIN 3	**73.35**
FILLER	**3.8**

TABLE A.8. *Bin percentage used for modified New Jersey (0% bin 2).*

COMPONENT	% Blend by Weight
BIN 1	**2.8**
BIN 2	**0.0**
BIN 3	**93.4**
FILLER	**3.8**

APPENDIX B. REVERBERATION ROOM TEST RESULTS

Presented in Figure B.1 and Figure B.2 are the results from the reverberation room tests. The empty room data and room with test sample data are shown in each figure, respectively. All fifty trials are plotted for each one-third octave band beginning at 125 Hz and proceeding through 2,500 Hz. Best-fit lines are drawn through the region of data used to calculate T_{60} for each band. The decay time and its standard deviation are also included on each graph.

A notable characteristic of the decay curves is the presence of a slight elbow bend in some of the higher frequency bands. This decay phenomenon is common for rooms with one or more absorptive surfaces. Typically, reverberation chambers have uniform reflective surfaces (usually concrete) to avoid the presence of this phenomenon. However, the chamber in ENS has a wooden lay-in ceiling with evenly spaced beams (16 in. periodicity) running parallel along the width of its exposed surface. All the other surfaces are smooth concrete. These beams may have introduced diffraction or preferential scattering at wavelengths corresponding to the periodicity, possibly causing some effect on the modal distribution and additional energy loss of the sound striking the ceiling. These losses may have been greater in the higher frequencies associated with the characteristic dimensions of the beams and beam spacing.

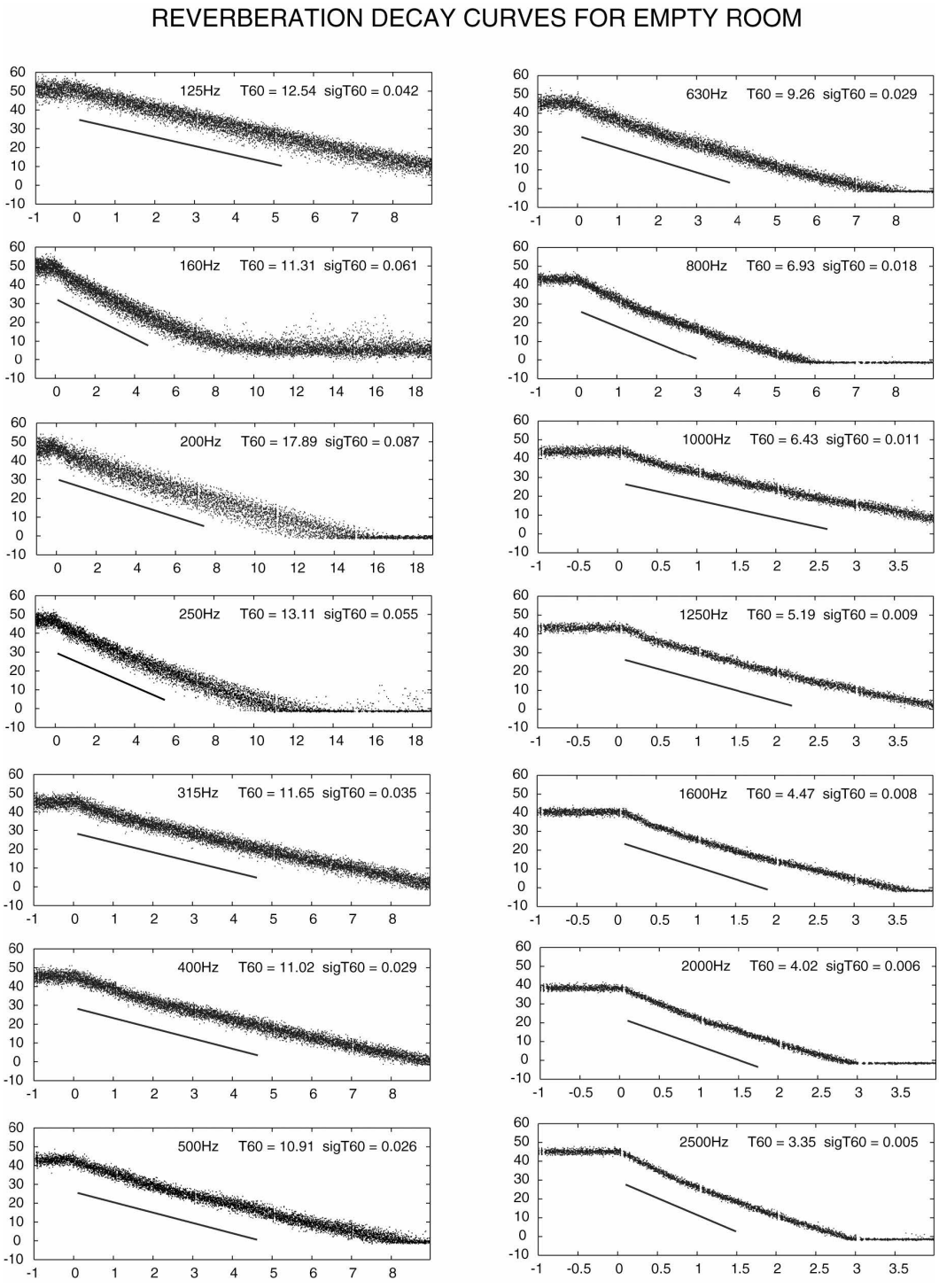

Figure B.1. Empty room decay curves plotted in dB versus time.

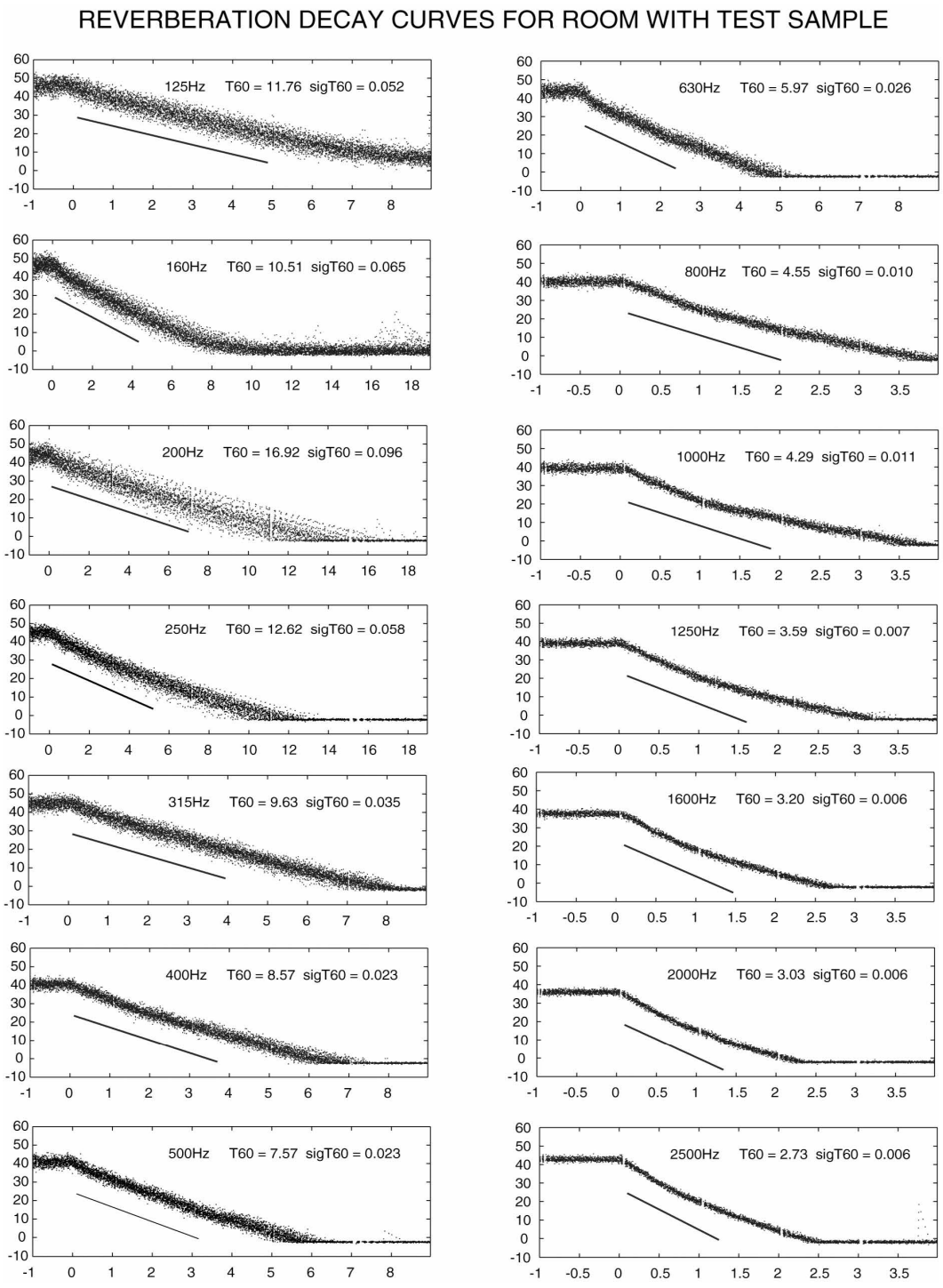

Figure B.2. Decay curves for room with sample plotted in dB versus time.

REFERENCES

[1] J. Kragh, "Traffic noise at porous asphalt road surfaces," *Inter-Noise 91,* 765-768 (1991).

[2] M. Berengier, J. F. Hamet, and P. Bar, "Acoustic properties of porous asphalts: Theoretical and experimental aspects," *Transportation Research Record 1265,* 9-24 (1991).

[3] M. McNerney, B. J. Landsberger, T. Turen, and A. Pandelides, "Comparative field measurements of tire pavement noise of selected Texas pavements," internal report for the Center for Transportation Research, The University of Texas at Austin (1997).

[4] G. V. Meij, "Noise generation on asphalt roads," Research Report RR 89/71/1, Research and Development Advice Committee, South African Roads Board, Department of Transportation, Pretoria (1991) [in Afrikaans].

[5] S. Iwai, Y. Miura, H. Koike, and G. Levy, "Influence of porous asphalt pavement characteristics on the horn amplification of tire/road contact noise," Inter-Noise 94, 431-434 (1994).

[6] K. Attenborough, "Acoustical characteristics of porous materials," Physics Reports 82, No. 3, 181-227 (1982).

[7] D. T. Blackstock, "Acoustics I," unpublished class notes (1997).

[8] L. M. Brekhovskikh and O. A. Godin, *Acoustics of Layered Media I,* Springer Ser. on Wave Phenomena, Vol. 5. (Springer, Berlin, 1990).

[9] J. Y. Chung and D. A. Blaser, "Transfer function method of measuring in-duct acoustic properties. I. Theory," *Journal of the Acoustical Society of America,* Vol. 68, No. 3, 907-913 (1980).

[10] ASTM E 1050, "Standard test method for impedance and absorption of acoustical materials using a tube, two microphones, and a digital frequency analysis system" (1990).

[11] ASTM C 384, "Standard test method for impedance and absorption of acoustical materials by the impedance tube method" (1998).

[12] ASTM C 423 REV A, "Standard test method for sound absorption and sound absorption coefficients by the reverberation room method" (1990).

[13] E. Irrgang, “Laboratory Report on ENS Reverberation Chamber Research for Reverberation Time,” unpublished memo to Mark Carpenter and E. L. Hixson (1998).

[14] L. L. Beranek, *Noise and Vibration Control* (McGraw Hill, New York, 1971).

[15] D. Nelson, interview at Acoustics Systems in Austin, Texas, March 9, 1999.

[16] P. R. Bevington and D. K. Robinson, *Data Reduction and Error Analysis for the Physical Sciences* (McGraw Hill, New York, 1992).

[17] D. Nelson, “On quantifying and using the ‘diffraction effect for cost-and-performance optimization of sound absorption treatments,” Noise-Con 90, 427-432 (1990).

[18] U. Sandberg, “Tire/road noise – studies of the mechanisms of noise generation, methods of measurement and road surface characterization,” Linköping Studies in Science and Technology, Dissertations. No. 166, Department of Physics and Measurement Technology Linköping University, Linköping (1987).